Inorg. Chem. **1985**, *24*, 4499–4503 **4499**

Contribution from the Department of Chemistry and Biochemistry,
University of California at Los Angeles, Los Angeles, California 90024

Single-Crystal Polarized Electronic Absorption Spectra and the Ligand Field Interpretation of the Bonding of the Trichloro(trimethylamine)platinate Ion

Tsu-Hsin Chang and Jeffrey I. Zink*

Received November 20, 1984

The single-crystal polarized spectra of $(Pr_4N)[PtCl_3NMe_3]$ taken at 10 K are reported. Spin-allowed and spin-forbidden ligand field transitions are assigned. The $d_{z^2} \rightarrow d_{x^2-y^2}$ transition is observed at high energy and is assigned. The spectra at 10 K and at room temperature are compared, and the temperature dependence of the energies and intensities of the bands are discussed. The spectra are compared to those of Cossa's salt, $PtCl_3NH_3^-$. A significant difference in the assignments of the $^1A_2$ band is discussed. The angular overlap parameters for the ligands are determined.

We have recently become interested in determining ligand field σ- and π-bonding parameters for ligands of importance in organometallic chemistry. A homologous series of compounds that has been yielding important information is $PtCl_3L^{n-}$. This series possesses the necessary attribute of having d–d bands, unencumbered by overlapping charge-transfer bands, which can be resolved and assigned from single-crystal absorption spectra. In addition, a large number of important ligands L including ethylene, CO, phosphines, isocyanides, and alkylidines can be coordinated to the $PtCl_3$ unit and are being studied. The first analysis of the bonding properties of one of these ligands, ethylene (in Zeise's salt), was recently reported.[1]

The σ- and π-interaction properties of ammonia and amines provide important reference points for interpreting the relative forward- and back-bonding properties of organometallic ligands. Ammonia is considered to be one of the strongest σ-bonding ligands and to have no π-bonding capabilities.[2-5] However, as will be discussed later, ammonia can have a significant effect on the energies of metal d orbitals of π symmetry. Also of interest to our studies is our finding that the reported σ-bonding parameter of ammonia in $PtCl_3NH_3^-$ is significantly lower than our values for the σ bonding of NMe_3 and ethylene.[6]

The σ-bonding parameter for a ligand L calculated from the electronic spectrum of a d^8 $PtCl_3L$ compound depends critically on the energy of the dipole-forbidden $^1A_2$ band (vide infra). In $PtCl_3NH_3^-$, this band is difficult to assign because it is obscured by a dipole-allowed transition.[6,7] One of our goals in this work was to find a salt of a $PtCl_3L$ compound containing a substituted amine in which better separation of the $^1A_2$ band from other ligand field bands occurs. $(Pr_4N)[PtCl_3N(CH_3)_3]$ possesses the desired property. A second goal in studying substituted amines was to locate the transition originating from the d_{z^2} orbital. The assignment of this transition in square-planar platinum complexes is controversial.[8-12] Amines will not produce low-lying charge-transfer bands that could obscure this d–d band.

In this paper we report the 10 K single-crystal polarized electronic absorption spectrum of $(Pr_4N)[PtCl_3N(CH_3)_3]$. Our microspectroscopic techniques enable us to measure the spectra of crystals tens of micrometers in length and breadth and 10^3 Å thick. Spin-allowed and spin-forbidden transitions are assigned. Ligand field theory is used to interpret the transition energies. The σ- and π-bonding parameters of the ligands are reported.

Table I. Peak Maxima and Assignments

bands at 10 K	bands at room temp	polarizn	assignt	label[c]
19 850	*a*	∥	triplet[b]	A
23 330	22 650	∥	triplet[b]	B
23 370	22 830	⊥	triplet[b]	B
27 490	26 070	⊥	triplet[b]	C
28 170	27 400	∥	$^1B_1$	C
32 710	31 600	∥, ⊥	$^1B_2$	E
34 850	32 880	⊥	$^1A_2$	F
38 540	38 120	∥	$^1A_1$	G

[a] Too broad to be observed. [b] Each band is comprised of several spin–orbit coupled components. See text and Table II for calculated state energies and assignments. [c] Label used in Figures 1 and 2.

Experimental Section

$(Pr_4N)[PtCl_3(N(CH_3)_3)]$ was prepared by the method of Goggin et al.[13,14] Single crystals were grown between quartz plates from an acetonitrile solution. A drop of the solution was placed on one plate and a second plate pressed over the first. The plates were stored in the dark. After several hours, long platelike crystals were obtained. When the crystals were examined under the polarizing microscope, one of the extinction axes was 2° from the long crystal axis. The parallel absorption spectra were taken with the electric vector of the incident radiation parallel to this extinction direction. The perpendicular spectra were obtained in the orthogonal extinction direction. Thin crystals were chosen for spectroscopic study. The ultrathin crystal was obtained by cleavage of a larger crystal when the quartz plates were separated.

The instrument that was used to obtain the crystal spectra is a locally constructed microspectrophotometer which has been described previously.[1] The solution phase spectra were recorded with a Cary 14 spectrophotometer.

Results

The polarized electronic absorption spectra of single crystals of $(Pr_4N)[PtCl_3N(CH_3)_3]$ obtained at 10 K are shown in Figures 1 and 2. The spectra in both figures were obtained from the same crystal face of different crystals having different thicknesses. One of the extinction axes is 2° from the long crystal axis. The parallel spectra were taken with the electric vector of the incident radiation parallel to the above extinction direction. The perpendicular spectra were obtained in the orthogonal extinction direction.

The energies of the peaks and shoulders are given in Table I. They are labeled A through G as shown in Figures 1 and 2. The spectral features fall into three categories: low-energy and low-intensity features A through C; medium-intensity and -energy features D through F, and the high-intensity highest energy peak G.

---

(1) Chang, T.-H.; Zink, J. I. *J. Am. Chem. Soc.* **1984**, *106*, 287.
(2) Perumareddi, J. R. *Coord. Chem. Rev.* **1969**, *4*, 73.
(3) Fee, W. W.; Harrowfield, J. N. MacB. *Aust. J. Chem.* **1970**, *23*, 1049.
(4) Keeton, M.; Chou, B. F.; Lever, A. B. P. *Can. J. Chem.* **1972**, *49*, 192.
(5) Glerup, J.; Monsted, O.; Schaffer, C. E. *Inorg. Chem.* **1976**, *15*, 1399.
(6) Francke, E.; Moncuit, C. *Theor. Chim. Acta* **1973**, *29*, 319.
(7) Fanwick, P. E.; Martin, D. S. *Inorg. Chem.* **1973**, *12*, 24.
(8) Martin, D. S. *Inorg. Chim. Acta, Rev.* **1971**, *5*, 107.
(9) Patterson, H. H.; Godfrey, J. J.; Khan, S. M. *Inorg. Chem.* **1972**, *11*, 2872.
(10) (a) Kroening, R. F.; Rush, R. M.; Martin, D. S.; Clardy, J. C. *Inorg. Chem.* **1974**, *13*, 1366. (b) Martin, D. S.; Tucker, M. A.; Kassman, A. J. *Inorg. Chem.* **1965**, *4*, 1682.
(11) Tuszynski, W.; Gliemann, G. *Z. Naturforsch., A: Phys., Phys. Chem., Kosmophys.* **1979**, *34A*, 211.
(12) Vanquickenborne, L. G.; Ceulemans, A *Inorg. Chem.* **1981**, *20*, 796.
(13) Goggin, P. L.; Goodfellow, R. J.; Reed, F. J. S. *J. Chem. Soc., Dalton Trans.* **1972**, 1298.
(14) Degner, M.; Pilbrow, M. F. *Transition Met. Chem. (Ukinheim, Ger.)* **1975/1976**, *1*, 41.

0020-1669/85/1324-4499$01.50/0 © 1985 American Chemical Society

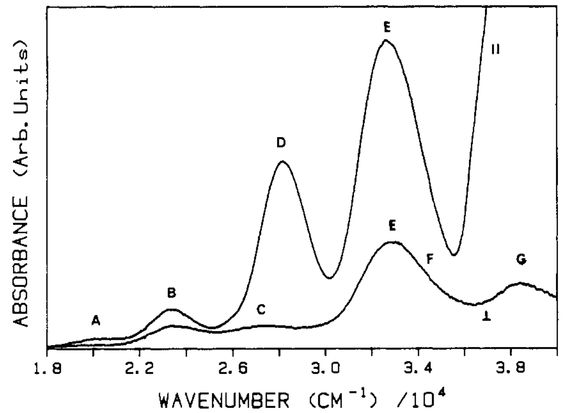

Figure 1. Single-crystal polarized electronic absorption spectrum of $(Pr_4N)[PtCl_3N(CH_3)_3]$ at 10 K: upper curve, the spectrum in parallel polarization; lower curve, the spectrum in perpendicular polarization.

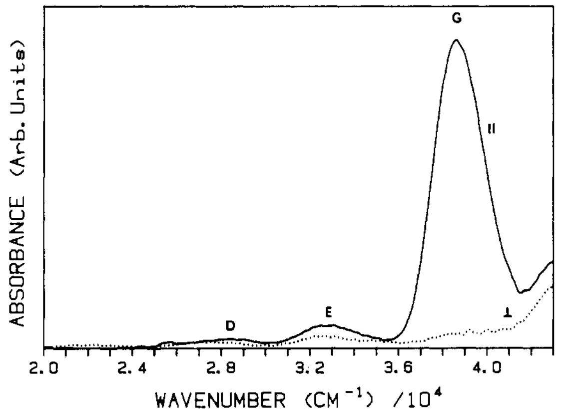

Figure 2. Ultrathin single-cyrstal polarized electronic absorption spectrum of $(Pr_4N)[PtCl_3N(CH_3)_3]$ at 10 K: solid line, parallel polarization; dotted line, perpendicular polarization.

The low-intensity features have maximum intensities of generally less than one-fifth of those of the higher intensity features. In the room-temperature solution spectrum, the broad, unresolved absorbance has a molar absorptivity of roughly 2 M^{-1} cm^{-1} in the 20 000–24 000-cm^{-1} region. The lowest energy feature that is resolved in the single-crystal polarized spectrum at 10 K, band A, appears in parallel polarization at 19 850 cm^{-1}. The second band, labeled band B, occurs at about 23 350 cm^{-1} in both polarizations but with lower intensity in the perpendicular direction. Band C is observed in perpendicular polarization at 27 490 cm^{-1}.

The remaining absorption features, bands D–G, play the most important role in the ligand field interpretation of the bonding (vide infra). Band D at 28 170 cm^{-1} is only observed in parallel polarization. Band E, at 32 700 cm^{-1}, is most intense in parallel polarization. Shoulder F, at about 34 850 cm^{-1}, is clearly evident on the high-energy side of band E in perpendicular polarization. Band G at 38 540 cm^{-1} is most intense in parallel polarization although a weak feature, probably resulting from incomplete extinction, is observed in perpendicular polarization. In room-temperature acetonitrile solution, band G has a molar absorptivity of 945 M^{-1} cm^{-1}.

The room-temperature electronic absorption spectra of the thicker of the two single crystals, taken under the same polarization conditions as those in Figure 1, are shown in Figure 3. The main features in the room-temperature spectra are similar to those in the 10 K spectra. However, all of the bands in the room-temperature spectra have a red shift and an increased bandwidth compared to the corresponding bands at low temperature. Band F in perpendicular polarization increased in intensity dramatically when the temperature was raised. The 10 K and room-temperature electronic absorption spectra of $(Pr_4N)[PtCl_3N(CH_3)_3)]$ in perpendicular polarization are shown on the same absorbance scale in Figure 4 in order to illustrate the large increase. The positions of the peaks and shoulders in the room-temperature spectra are given in Table I and are labeled the same as those in the 10 K spectra.

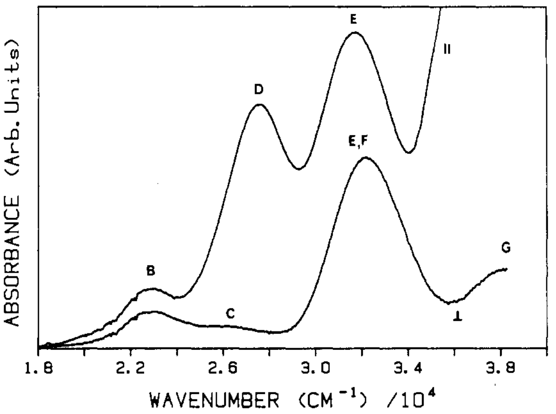

Figure 3. Single-crystal polarized electronic absorption spectrum of $(Pr_4N)[PtCl_3N(CH_3)_3]$ at room temperature: (∥) parallel polarization; (⊥) perpendicular polarization.

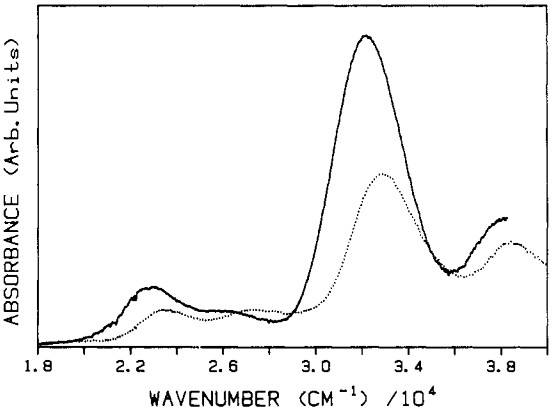

Figure 4. Temperature effect of the single-crystal polarized electronic absorption spectrum of $(Pr_4N)[PtCl_3N(CH_3)_3]$ in perpendicular polarization: solid line, room temperature; dotted line, 10 K.

Discussion

1. Assignments of the Transitions. The bands in Figures 1–3 are categorized and assigned in three groups: singlet d–d transitions, triplet d–d transitions, and the d_{z^2} transition. The medium-intensity bands D–F, which we assign as singlet d–d transitions, are very similar to those of $PtCl_3NH_3^-$, which were assigned by Martin et al.[7] and Monciut et al.[6] on the basis of the polarization properties, and to those of $PtCl_3(C_2H_4)^-$, which were assigned by us on the basis of the polarization properties.[1] The most significant difference between the spectra and assignments of the NH_3 and the NMe_3 complexes is the temperature-dependent band in Figure 4. This band is discussed in detail below. A minor difference between the spectra is the small red shift of the bands in the NMe_3 complex compared to those in the NH_3 complex. A red shift is expected in $PtCl_3NMe_3^-$ because NMe_3 is expected to be lower in the spectrochemical series than NH_3. Because of the similarity between the spectra, our assignments of the singlets parallel those previously made for the above $PtCl_3L^-$ complexes. The polarization properties are primarily used in this study to resolve and separate the bands. They can only be indirectly used to assign the bands because the crystal structure is not known.

The "triplet" bands are assigned primarily by using ligand field theory. These bands can never be readily assigned solely from their polarization properties, even when full crystallographic data are known, because their intensities are very sensitive to their couplings to singlet states.[1,7] Furthermore, our spin–orbit coupling treatment shows that the observed maxima are a superposition of clusters of closely spaced spin–orbit coupled components of "triplet" states. (In the C_{2v} point group, each "triplet state" consists of three components; i.e., $^3A_1$ transforms as $A_2 + B_1 + B_2$.) The

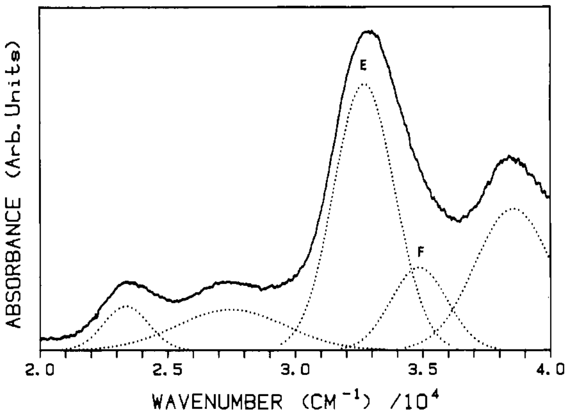

Figure 5. Gaussian fit of the single-crystal polarized electronic absorption spectrum of $(Pr_4N)[PtCl_3N(CH_3)_3]$ at 10 K in perpendicular polarization: solid line, observed spectrum; dotted line, the individual Gaussian peaks.

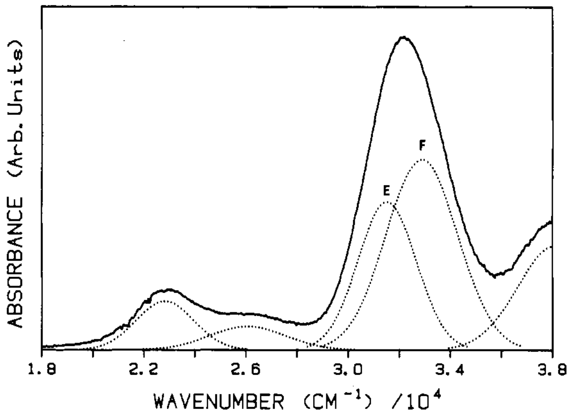

Figure 6. Gaussian fit of the single-crystal polarized electronic absorption spectrum of $(Pr_4N)[PtCl_3N(CH_3)_3]$ at room temperature in perpendicular polarization: solid line, observed spectrum; dotted lines, the individual Gaussian peaks.

details of the triplet states will be discussed below in terms of the ligand field calculations, including spin–orbit coupling.

The assignment of the highest energy band, which has not previously been observed in single-crystal spectra, is discussed in terms of the mysterious transition from the d_{z^2} orbital, the assignment of which is controversial in the spectra of platinum (II) complexes.[8-12] Both its experimentally observed polarization and its ligand field theoretical energy are considered.

The molecular axis system that is used in this paper is the "chemists" axis system in which the *z* axis is perpendicular to the square plane and the *x* axis lies along the metal–nitrogen bond. Details of the axis system and the selection rules were discussed previously[1] and will not be repeated here.

Singlet States. Four spin-allowed transitions are expected, three of which are electric dipole allowed and one of which is only vibronically allowed.[1,7] Two of the dipole-allowed transitions are assigned by directly applying the band assignments from the NH_3 compound.[7] Band D is the $^1A_1 \rightarrow {}^1B_1$, $d_{xy} \rightarrow d_{x^2-y^2}$ transition and band E is the $^1A_1 \rightarrow {}^1B_2$, $d_{xz} \rightarrow d_{x^2-y^2}$ transition. These bands were observed at 29 400 and 33 700 cm^{-1}, respectively, in the spectrum of the NH_3 compound.[7] (Note that the axis system used in ref 7 is different from that used in ref 1 and in this work.) The remaining dipole-allowed band, $^1A_1 \rightarrow {}^1A_1$, $d_{z^2} \rightarrow d_{x^2-y^2}$, which has not been identified in square-planar platinum (II) complexes, will be discussed in conjunction with band G.

The dipole-forbidden, vibronically allowed band cannot be assigned by analogy to the ammonia complex. This band is expected to be weaker than the dipole-allowed bands, to exhibit a large temperature dependence, and to be close in energy to the $^1B_2$ band. Band F exhibits all of these properties. In the 10 K spectrum (Figure 1) band F is the shoulder on the *high*-energy side of band E. It is most obvious in perpendicular polarization where the overlapping band E, the $^1B_2$ transition, is partially extinguished.

In the room-temperature perpendicular-polarized spectrum (Figure 3) band E and shoulder F have the appearance of a single band that is increased in relative intensity, increased in width at half-height, and *blue* shifted. These observations are explained by a large increase in the intensity of band F, which, when overlapped with band E, produces what appears to be a single broader band with its maximum intermediate in energy between the two components.

The positions and intensities of the two components were determined by carrying out a Gaussian fit of the spectra. The decomposed peaks in the perpendicular polarization spectrum at 10 K and at room temperature are shown in Figures 5 and 6, respectively. The fitted position of the peak maximum of band E at room temperature is 31 522 cm^{-1}, and at 10 K it is 32 712 cm^{-1}. These values are almost identical with the observed peak maxima of band E in parallel polarization, 31 600 and 32 700 cm^{-1} respectively, at the corresponding temperatures. Furthermore, the fitted intensities of band E at room temperature and at 10 K are equal within experimental error. The results imply that band E is a dipole-allowed band and provide further support for the assignment of band E to the $^1A_1$ to $^1B_2$, $d_{xz} \rightarrow d_{x^2-y^2}$ transition. The intensity of the fitted band F is over 4 times greater at room temperature than that at 10 K. This dramatic temperature effect supports the assignment of band F to the vibronically allowed $^1A_1 \rightarrow {}^1A_2$, $d_{xy} \rightarrow d_{x^2-y^2}$ transition.

The assignment is supported by the magnitude of the intensity increase with increasing temperature. The temperature dependence of the intensity of a dipole-forbidden band that becomes allowed by coupling with a vibration is

$$I(T) \propto \coth\,(h\nu/2kT)$$

where $h\nu$ is the energy of the vibrational mode, k is the Boltzmann constant, and T is the temperature.[15] The observed fourfold increase in intensity requires that $h\nu \sim 300$ cm^{-1}. Pt–Cl stretching frequencies are found between 300 and 330 cm^{-1} in similar compounds.[16,17] The good agreement supports the dipole-forbidden, vibronic allowed $^1A_2$ assignment. More detailed temperature-dependence studies were not carried out because of the inherent uncertainties in the Gaussian fitting procedures.

The d_{z^2}, $^1A_1$ Transition. Standard ligand field theory, in both its *Dq*, *Ds*, *Dt*, and angular overlap model (AOM) formalisms, predicts that the $d_{z^2} \rightarrow d_{x^2-y^2}$ transition is one of the *lowest* energy one-electron d–d transitions in square-planar complexes.[12,18] In a careful study of a square-planar first-row transition-metal complex of Cu(II), Hitchman et al.[19] identified this tranisition as the *highest* energy d–d transition. Moncuit et al.[6] have proposed that a new LF parameter representing s–d mixing[20,21] be used to explain the high energy of the transition.

A high-energy band, which has not previously been observed in crystal spectra of tetrahaloplatinates or substituted haloplatinates, is observed in the spectrum of the ultrathin crystal shown in Figure 2 (band G). We tentatively assign this band to the $^1A_1 \rightarrow {}^1A_1$, $d_{z^2} \rightarrow d_{x^2-y^2}$ transition, but note that an alternative assignment to a spin-forbidden chloride to platinum charge-transfer transition cannot be completely eliminated.[22]

The intensity of band G is within the region of a dipole-allowed d–d transition of a third-row transition-metal complex. In CH_3CN

---

(15) Ballhausen, C. J. "Introduction to Ligand Field Theory"; McGraw-Hill: New York, 1962; p 187.

(16) Adams, D. M. "Metal-Ligand and Related Vibrations"; Edward Arnold Ltd.: London, 1967.

(17) Poulet, H.; Delorme, P.; Mathieu, J. P. *Spectrochim. Acta* **1964**, *20*, 1855.

(18) Fenske, R. F.; Martin, D. S.; Ruedenberg, K. *Inorg. Chem.* **1962**, *1*, 441.

(19) Hitchman, M. A.; Cassidy, P. J. *Inorg. Chem.* **1979**, *18*, 1745.

(20) Basch, H.; Gray, H. B. *Inorg. Chem.* **1967**, *6*, 365.

(21) Cotton, F. A.; Harris, C. B. *Inorg. Chem.* **1967**, *18*, 1745.

(22) The band at about 36 500 cm^{-1}, which has been observed in the solution and reflectance spectra of the $PtCl_4{}^{2-}$ ion, has been attributed by some authors to the $d_{z^2} \rightarrow d_{x^2-y^2}$ transition: Chatt, J.; Gamlen, G. A.; Orgel, L. E. *J. Chem. Soc.* **1958**, 486. Day, P.; Orchard, A. F.; Thompson, A. J.; Williams, R. J. P. *J. Chem. Phys.* **1965**, *42*, 1972.

solution, it has an extinction coefficient of 945 M^{-1} cm^{-1}. It is more intense than the other d–d transitions, but intensity borrowing from nearby CT transitions are likely. Its energy, 38 119 cm^{-1}, is much lower than the 45 300-cm^{-1} chloride to metal charge-transfer transition observed in $PtCl_3NH_3^-$.[7]

Other properties of band G are consistent with a $d_{z^2} \rightarrow d_{x^2-y^2}$ transition. The band width at half-height is about the same as those of the other d–d bands. The red shift and the magnitude of the shift as the temperature is raised are essentially the same as those of the other d–d bands. Its polarization, i.e. allowed in parallel polarization, is also consistent. Experience with $PtCl_3L^-$ compounds has shown that when the $^1B_1$ band extinguishes completely in one polarization (here perpendicular polarization), that direction is primarily along the molecular *z* axis. Thus, parallel polarization contains in general both *x* and *y* components. The $^1A_1 \rightarrow {}^1A_1$ transition, which is *x*-allowed and *z*-forbidden, should have the polarization properties shown by band G.

2. Calculation of the Transition Energies and the Ligand Field Parameters. Calculations of the d–d transition energies usually use one of two forms of ligand field theory, the angular overlap model (AOM)[1,6,12] or the traditional form in terms of parameterized radial integrals *Dq*, *Ds*, and *Dt*.[18] The two forms are interrelated.[23] In this paper, the AOM model will be used because the resulting parameters have a greater appeal in terms of interpreting trends in bonding properties.

In a straightforward application of the original AOM to $PtCl_3L$ complexes, there are seven parameters to be evaluated: the σ- and π-bonding parameters for the chloride, e_σ^{Cl} and e_π^{Cl}, the σ- and π-bonding parameters for the ligand L (in this case the amine), e_σ^{N} and e_π^{N}, the Racah parameters *B* and *C*, and the spin–orbit coupling parameter ζ. Thus in the case of $PtCl_3NMe_3^-$, where there are seven observed bands and seven parameters, an exact solution is possible. Unfortunately, as discussed previously, ligand field theory is incapable of correctly treating the transition from the d_{z^2} orbital. This problem can be quantitatively treated by introducing a parameter to account for mixing of the 6s and 5d orbitals. This parameter was introduced by Moncuit in a complicated form[6] and later rewritten in a simplified form as e_{sd}.[12] With the addition of this parameter, there are eight parameters and seven observables, making an exact solution impossible. If a further refinement, which allows for the different magnitudes of π interactions in the plane, $e_\parallel$, and out of the plane, $e_\perp$, are included for both the chloride and ammine ligands, a total of ten parameters are introduced. Again, an exact solution is impossible.

The number of variable parameters is usually reduced in ligand field calculations by making a series of approximations, such as the approximation that parameters for a given ligand can be transferred between compounds, that *B* and *C* have a fixed ratio, etc. The strategy that will be adopted in this and the following works will be to use a minimum number of approximations, and to use those approximations that will least affect the ligand field parameters for the unique ligand L. In the calculations that follow, the most refined of the above calculations is used with the following two approximations: the parameters for the chloride ligand and for the spin–orbit coupling constant are transferrable between similar compounds within uncertainties of about 500 and 100 cm^{-1}, respectively. By using these two approximations, the number of variable parameters is reduced from ten to six, the number of observables is seven, and an "exact" solution is possible.

The results of the full ligand field calculation including spin–orbit coupling are given in Table II. The matrix elements given by Moncuit et al.[6] and the parameters given at the bottom of the table were used. Excellent agreement between the calculated and observed transition energies is obtained.

The calculated transition energies for the singlet states agree with those observed with an average discrepancy of only 185 cm^{-1}. Furthermore, the identities of the states giving rise to the calculated transitions agree exactly with the assignments discussed previously. A significant aspect of the calculation is that the energy of the transition originating from the d_{z^2} orbital is accurately calculated when an e_{sd} parameter is used that represents equal stabilization of d_{z^2} by s–d mixing and destabilization of the orbital by the ligand field.[12]

Table II. Calculated and Observed Transition Energies[a]

calcd	obsd	assignt	label
Singlets			
28 061	28 170	$^1B_1$	D
32 729	32 700	$^1B_2$	E
34 882	34 850	$^1A_2$	F
39 120	38 540	$^1A_1$	G
Triplets			
19 342		A_1	
19 547	19 850	A_2	A
19 925		B_1	
20 929		B_2	
22 609		B_1	
22 655	23 330 (∥)	A_2	B
23 143	23 370 (⊥)	A_1	
23 591		B_2	
25 116	*b*	A_1	*b*
27 111	27 490	B_2	C
27 277		A_2	
29 625	*b*	B_1	*b*

[a] The transition energies were calculated by using the following parameters (cm^{-1}): $e_\sigma^{Cl} = 11\,800$, $e_{\pi,\parallel}^{Cl} = 3000$, $e_{\pi,\perp}^{Cl} = 2700$, $e_\sigma^{N} = 21\,700$, $e_{\pi,\parallel}^{N} = 4600$, $e_{\pi,\perp}^{N} = 5600$, $e_{sd} = 16\,750$, $B = 690$, $C = 2700$, $\zeta = 2780$. The π parameters have in-plane (∥) and out of plane (⊥) components. The mean value is discussed in the text. [b] In the experimental spectrum, nonzero intensity without a well-defined peak or shoulder is observed.

The calculated triplet state transition energies also agree well with the observed band positions although, as expected, there is not a one to one correspondence. For example, band A is formed by the superposition of a cluster of four states. The irreducible representations of these states are given in Table II. Each of them is a spin–orbit coupled component of a parent "triplet" state. Band B is also formed from a cluster of four components, and band C is formed from two components. The calculated energies of two of the states fall between well-defined experimental peaks in Figure 1. It is interesting to note that their calculated positions do lie in regions where nonzero intensity is observed. These results dramatically illustrate why the polarization properties alone cannot be used to assign an observed band in an experimental spectrum to a given triplet state such as $^3B_1$.

The ligand field AOM parameters calculated for NMe_3 differ significantly from those reported for NH_3.[6,12] The value of e_σ^{N}, which represents the σ donation to the platinum from the nitrogen, is 21 700 cm^{-1} for NMe_3 according to the calculation discussed above and between 14 300 and 15 629 cm^{-1} for NH_3 according to published reports. The value of e_π^{N} is 5100 cm^{-1} for NMe_3 and is 1700 cm^{-1} or an assumed zero for NH_3. The values of both of the parameters for NMe_3 are larger, not smaller as expected, than those for NH_3.

The reason for the unexpectedly large difference between the σ value reported for NH_3 and that determined for NMe_3 in this paper is the assignment of the $^1A_2$ band. As discussed previously, the value of e_σ^{N} is extremely sensitive to the energy of the $^1A_2$ band. On the basis of the spectrum in Figure 1 and the temperature effects, we assign the $^1A_2$ band to the shoulder on the *high*-energy side of the $^1B_2$ band, which increases in intensity when the temperature is raised from 10 to 300 K. In the ammonia complex, the $^1A_2$ band was assigned to a feature *lower* in energy than the $^1B_2$ band. Thus the reported value of e_σ^{N} is lower for NH_3 than our value for NMe_3.

The meaning of the π parameters for ammines is a source of confusion. Because ammonia is usually considered to interact only in a σ fashion with metals, a reasonable and widely used assumption is to define $e_\pi^{N} = 0.0$. When the value of e_π^{N} is determined by a fitting procedure, it assumes a positive value.[12] We interpret the nonzero value as a manifestation of the electrostatic

---

(23) Lever, A. B. P. *Coord. Chem. Rev.* **1982**, *43*, 63.

interaction between the lone pair on the nitrogen with the metal d orbitals. Thus in the square-planar complexes, both the d_{xy} and the d_{xz} orbitals are raised in energy by the electrostatic interaction, leading to the nonzero values.

Summary

Ligand field electronic absorption transitions, including the d_{z^2} to $d_{x^2-y^2}$ transition and the spin-forbidden transitions, have been assigned in the low-temperature single-crystal polarized absorption spectra. The dipole-forbidden $^1A_2$ band shows the temperature dependence expected of a vibronic excitation. The angular overlap parameters show that NMe_3 is a strong σ donor and that its influence on the d orbitals of π symmetry through a proposed electrostatic interaction is significant.

Acknowledgment. The support of the National Science Foundation and the U.S. Army Research Office is gratefully acknowledged.

Registry No. $(Pr_4N)[PtCl_3(N(CH_3)_3)]$, 37084-09-6; $PtCl_3NMe_3^-$, 44630-47-9.

Contribution from the Department of Chemistry,
North Dakota State University, Fargo, North Dakota 58105

On the Observability of Cubic P_8

Michael W. Schmidt* and Mark S. Gordon*

Received June 27, 1985

A recent MNDO calculation predicts that the hypothetical P_8 is more stable than the observed gas-phase species P_4. The ab initio calculations reported here predict just the opposite but do establish that P_8 is more stable than another experimentally known form, P_2. The relative enthalpies (kcal/mol) are found to be as follows: $4P_2$, 72.4; $2P_4$, 0; P_8, 30.4. A force field analysis proves P_8 has a cubic structure. The bond length, vibrational frequencies, and photoelectron spectrum of P_8 are predicted.

Introduction

Just above its sublimation temperature of 704 K, phosphorus exists as tetrahedral P_4. Heating of the gas causes dissociation to diatomic molecules. These are the only two species identified at temperatures up to 1470 K.[1] Another possible allotrope, P_8, has never been conclusively identified.

P_8 is generally assumed to possess a cubic structure. The right angles in this configuration are close to the natural angles for phosphorus. For example, PH_3 has bond angles of 93.3°.[2] The relief of ring strain compared to $2P_4$ certainly makes cubic P_8 plausible.

A few polyphosphorus ionic species are known. P_8^{2+} has been claimed to be responsible for the blue color of solutions of phosphorus in disulfuric acid.[3] P_8^+ was detected by a mass spectrometer[4] in the vapor of subliming amorphous red phosphorus. This ion was present at 0.5% of the intensity of P_4^+, which would indicate that neutral P_8 was present in the vapor. A subsequent similar mass spectrometry experiment[5] failed to see any P_8^+, establishing an upper limit of 0.00002 for the relative intensities of P_8^+ to P_4^+. (This later experiment did, however, detect As_8^+). A number of crystals containing the P_7^{3-} anion are known. The crystal structure[6] shows this anion consists of a nortricyclene structure. P_{16}^- consists of two such nortricyclene systems, joined by a bridging P_2 group,[7] rather than containing two P_8 units.

A recent communication by Halevi, Bock, and Roth[8] reported that the elemental modification P_8 is much more stable than two P_4 molecules, by 68 kcal/mol, according to MNDO calculations. However these authors speculated that P_8 is unobservable because the D_{3d} symmetry dimerization is Woodward–Hoffmann forbidden. Since alternative synthetic routes are certainly conceivable, their prediction of thermodynamic stability for P_8 is the main result and conflicts with two earlier ab initio studies.

The previous ab initio investigations of P_8 employed two different pseudopotential methods. Fluck, Pavlidou, and Janoschek[9] used an assumed bond length of 2.21 Å for both P_4 and P_8, and found P_8 to lie 47 kcal/mol above two P_4 molecules. Trinquier, Malrieu, and Daudey[10] did perform geometry optimization of the two species and found P_8 to lie 10 kcal/mol below two P_4. However, these authors stated that the incorporation of d orbitals in their calculations would probably reverse this conclusion.

The full weight of quantum chemistry has not yet been brought to bear on the $4P_2/2P_4/P_8$ system, because of its large size. For example, none of the previous theoretical investigations of P_8 used d orbitals on phosphorus. One of the calculations did not optimize the geometry. No one has checked the assumption that P_8 has a cubic structure. We describe here all electron ab initio calculations in extended basis sets that should help to resolve the current ambiguity concerning the relative energies of $2P_4$ and the as yet unobserved P_8. In addition, we report vibrational frequencies and ionization potentials for P_8 to assist in its experimental identification.

Theoretical Procedure

Geometry optimizations were performed on P_2, P_4, and P_8 with three types of basis sets. The minimal STO-2G and STO-3G bases[11] are used for comparison with the MNDO calculation,[8] since this is essentially a parameterized minimal basis calculation. As will be shown, the STO-NG bond lengths are reasonably good, especially compared to the very short MNDO bond lengths. The split-valence 3-21G basis[12] gives results comparable to those of the pseudopotential calculations,[10] including very long bond lengths. These long bond lengths are overcome by using the

---

(1) Bock, H.; Muller, H. *Inorg. Chem.* **1984**, *23*, 4365–4368.

(2) Herzberg, G. "Electronic Spectra of Polyatomic Molecules"; Van Nostrand Reinhold: New York, 1966; p 610.

(3) Paul, R. C.; Puri, J. K.; Malhotra, K. C. *J. Chem. Soc., Chem. Commun.* **1971**, 1031–1032.

(4) Kerwin, L. *Can. J. Phys.* **1954**, *32*, 757–758.

(5) Kane, J. S.; Reynolds, J. H. *J. Chem. Phys.* **1956**, *25*, 342–349.

(6) von Schnering, H. G.; Menge, G. *Z. Anorg. Allg. Chem.* **1981**, *481*, 33–40.

(7) von Schnering, H. G.; Manriquez, V.; Honle, W. *Angew. Chem., Int. Ed. Engl.* **1981**, *20*, 594–595.

(8) Halevi, E. A.; Bock, H.; Roth, B. *Inorg. Chem.* **1984**, *23*, 4376–4378.

(9) Fluck, E.; Pavlidou, C. M. E.; Janoschek, R. *Phosphorus Sulfur* **1979**, *6*, 469–474.

(10) Trinquier, G.; Malrieu, J.-P.; Daudey, J.-P. *Chem. Phys. Lett.* **1981**, *80*, 552–557.

(11) Hehre, W. J.; Ditchfield, R. F.; Stewart, R. F.; Pople, J. A. *J. Chem. Phys.* **1970**, *52*, 2769–2773. The valence scale factor used is 1.74: Marsh, F. J.; Gordon, M. S. *Chem. Phys. Lett.* **1977**, *45*, 255–260.

(12) (a) Gordon, M. S.; Binkley, J. S.; Pople, J. A.; Pietro, W. J.; Hehre, W. J. *J. Am. Chem. Soc.* **1982**, *104*, 2797–2803. (b) Binkley, J. S.; Pople, J. A.; Hehre, W. J. *J. Am. Chem. Soc.* **1980**, *102*, 939–947.

0020-1669/85/1324-4503$01.50/0